Fermi National Accelerator Laboratory

FERMILAB-Conf-94/310-E

Perturbative QCD Tests from the LEP, HERA, and Tevatron Colliders

Stephen Kuhlmann

Fermi National Accelerator Laboratory
P.O. Box 500, Batavia, Illinois 60510

September 1994

To be *Submitted to the XIV International Conference of Physics in Collision,* Tallahassee, Florida, June 15-17, 1994

Operated by Universities Research Association Inc. under Contract No. DE-AC02-76CHO3000 with the United States Department of Energy

Disclaimer

CDF/PUB/JET/PUBLIC/2800
Aug 29, 1994

FERMILAB-CONF-94/310-E

PERTURBATIVE QCD TESTS FROM THE LEP, HERA, and TEVATRON COLLIDERS

Stephen Kuhlmann
Argonne National Laboratory

Abstract

A review of QCD tests from LEP, HERA and the TEVATRON colliders is presented. This includes jet production, quark/gluon jet separation, quark/gluon propagator spin, α_s updates, photon production, and rapidity gap experiments.

To be submitted to the XIV International Conference on Physics in Collision, Tallahassee, Florida, June 15-17, 1994

1 Introduction

Perturbative QCD is generally accepted as a successful model of the strong interactions, but has not had the precise, definitive tests such as QED. The success of the model stems from a large body of experimental tests in deep inelastic lepton-hadron scattering, electron-positron collisions, and hadron-hadron collisions. Just in the last year these three areas have reached new levels of precision and explored kinematic regions never tested before. In general these have confirmed QCD as a successful model, but many times as the precision improves disagreements appear between experiment and theory which help us understand the technical difficulties of the model as well. This paper will illustrate some of the successes as well as a few of the disagreements between experiment and QCD predictions. A new era in the push into the boundary between perturbative and non-perturbative QCD is also beginning, as shown by the rapidity gap experiments at HERA and the TEVATRON which may reveal the structure of the pomeron.

2 Jet Production and Quark/Gluon Jet Separation

Jet production is an excellent testing ground for QCD, as jets are produced abundantly at ep, e^+e^-, and hadron colliders, and in many different ways. They will be used extensively in the α_s measurements discussed later. Jet counting at all 3 different colliders is a direct probe of the coupling strength, as well as a direct measurement of the number of gluons inside the proton at the hadron colliders. QCD also predicts differences between the internal properties of quark and gluon jets, and improved evidence for this is presented.

We begin with inclusive jet production at the TEVATRON. Jets are produced dominantly at low P_T (15 GeV) by the t-channel gluon-gluon scattering, while at middle P_T values (100 GeV) quark-gluon initial states are largest, then at the highest P_T values (400 GeV) quark-quark initial states dominate. Thus the inclusive jet cross section from 15-450 GeV tests a variety of scattering diagrams as well as a variety of different parton densities over a wide range of Feynman x values. Of order 1 million jet events have been recorded by CDF and D0 spanning 9 orders of magnitude in cross section, and at the same time the NLO QCD predictions have very small scale dependences, leading to precise comparisons. This is shown in figure 1 from the D0 experiment for both central jets and forward produced jets, using the jet cone algorithm. This is the inclusive jet cross section versus jet energy transverse to the beam direction. The solid lines are the QCD predictions, the dashed lines represent the preliminary systematic uncertainties. The agreement with the data is remarkable, even more so when the CDF measurement is shown on a linear scale in figure 2. The agreement to within 20% over 9 orders of magnitude in cross section is one of the most impressive successes of QCD. The data and theory are also now precise enough to severely constrain the number of gluons in the proton.

One of the most important QCD tests of the last year is the rise of F_2 at small-x at HERA, indirectly predicted by the resummation of large logarithms such as ln(1/x). This was summarized in a separate talk at this conference, thus I will not discuss it here, instead I will briefly discuss jet production at HERA now and then rapidity gaps from HERA in more detail later. At the born level at HERA a quark is scattered from the proton, giving rise to a single jet plus the proton remnant. Two-jet production (plus the proton remnant) arises when that quark emits a gluon in either the initial or final states, or when a gluon splits into a quark pair and one of the quarks is scattered(photon-gluon fusion). Figure 3 shows two-jet production from the Zeus experiment, compared to two QCD predictions. The dashed line is the prediction using only the 2 matrix elements discussed above for two-jet production, whereas the solid line includes the born diagram plus a full parton shower, in addition to the two-jet matrix elements. Clearly the full prediction does an excellent job of predicting the energy and angular dependences of two-jet production at HERA. In fact, the ratio of 2-jet/1-jet events has been used by H1 in a preliminary measurement of α_s .

With the CM energy fixed in e^+e^-collisions, the emphasis of jet production shifts away from energy distributions towards multi-jet fractions, event shapes, etc. Multi-jet production in e^+e^-collisions is a classic test of QCD and the coupling constant strength. This is shown in figure 4, with multi-jet fractions and predictions for both LEP and PEP energies, using the E0 jet clustering. The lines are not fits to the data, they are predictions using the JETSET QCD shower monte carlo. Note the data and predictions for the fraction of three-jet events. For a certain value of ycut, the PEP data is higher than the LEP data, this is due to the smaller CM energy leading to a larger α_s , which produces more three-jet events.

As mentioned above, QCD predicts the internal structure of quark and gluon jets to be different, namely quark jets are more collimated and with a smaller multiplicity. The OPAL experiment reanalysed their data with the same cone algorithm used by CDF, and compared the resulting jet shapes with the published CDF data, at the same jet energy. This is the first time such a comparison has been possible. The point is that both samples are believed to be more than 80% pure, meaning the LEP data is more than 80% quark jets, and the CDF data is more than 80% gluon jets. The comparison is shown in figure 5. The data points are the integrated fractional energy measured in a sub-cone inside the jet. For example the data show that 90% of the jet energy is contained within a cone 0.4 for OPAL quark jets, while 75% of the jet energy is contained within a cone 0.4 for CDF gluon jets. There is a long history in the study of quark and gluon jets, but this is the most impressive difference between the two I have seen.

3 Quark/Gluon Propagator Spin

One of best pure tests of QCD in hadron collisions are the angular distributions of the two-parton final state. The processes with a quark propagator (spin 1/2) such as direct photons or W production give rise to a fairly flat angular distribution in the CM frame, while processes with a gluon propagator (spin 1) such as dijet production are highly peaked in the forward direction. A summary of these is shown in figure 6, for dijets, photons and Ws at CDF. The distinction between the different processes and the agreement with QCD predictions is clear. D0 with its excellent forward calorimetry has extended the dijet measurement another 2 orders of magnitude, this is shown in figure 7 along with LO QCD predictions with and without a running α_s .

4 α_s Measurements

In the last year significant improvements have taken place in the measurements of α_s . The LEP Z branching fraction into hadrons experimental error has been reduced and new papers on the theoretical errors have been published, making this a very competitive and clean measurement of α_s . Resummed calculations of some of the LEP event shape measurements are now available, reducing the scale dependence but typically are only available in regions where hadronization effects are largest, thus the total theoretical uncertainty is not greatly improved. Nevertheless the agreement between these measurements and previous ones is encouraging. For more information on this I refer you to Siggi Bethke's review [1]. The debate about theoretical uncertainties in tau decays continues, while H1 and D0 have new measurements using ratios of jet counts. Figure 8 summarizes the world's measurements on α_s evaluated at the Z mass, showing amazing agreement with many different processes, this plot is clearly the one that demonstrates best the validity of QCD as the model of the strong interactions. Perhaps the second best plot to demonstrate QCD success is figure 9, which shows the running of α_s with the different measurements at different scales.

5 Photon Production

Direct photon production in hadron collisions is attractive due to the initial state gluon in the compton scatter, but photons are also produced by fragmenting off a quark. This is the process that gives rise to direct photons at LEP, and LEP data can give useful input into our understanding of the fragmentation process in hadron collisions. We begin by presenting the measured cross sections from CDF and D0, in figure 10. The NLO QCD prediction (including the fragmentation process) agrees qualitatively with the data sets. We also find good agreement between matrix-element predictions of photon production at OPAL, and the data as shown in figure 11. The data from hadron collisions now span a wide x-range, from .013 to .55, and could provide a significant constraint on the gluon density in this range. A global parton distribution fit to fixed target and collider direct photon data, as well as the normal DIS and Drell-Yan data sets, has been attempted by using the CTEQ global analysis package [2], with the results being shown in the next two figures. We display this versus photon Xt ($2P_T/\sqrt{s}$) in order to survey the entire x-range at once. Figure 12 shows this from the CDF, UA2, R806(ISR), and E706 experiments, while figure 13 has a blowup of the fixed target region including now UA6 and WA70 data. The small errors for the CDF experiment mean it tends to dominate the fit, and increase the gluon densities in its x-range. But a noticeable trend seems to emerge, with all the data sets having an excess of photons at low P_T, rather than in any specific x-range. Thus it is hard to imagine a change in parton densities that can account for this. The ISR and fixed target data are also insensitive to fragmentation processes, thus it is difficult to derive an explanation for all the data based on this. One possibility is that the NLO QCD prediction does not have enough of a photon-jet system "kt kick" due to initial state gluon radiation, this would affect the low P_T end of each measurement. It is known that for diphoton production at CDF, the NLO QCD prediction for the diphoton system "kt kick" is significantly smaller than QCD shower monte carlos that have multiple initial state gluon emissions. One reason this effect may have not been seen before is due to the emphasis placed on the WA70 data in previous analyses, and one can see in figure 13 that their data is consistent with being flat(no effect), while at the same time within errors the WA70 data agrees with UA6 and E706, which do show a slope somewhat different than QCD.

6 Rapidity Gap/Pomeron Measurements

New measurements from HERA, as well as the TEVATRON, have opened up the field of hard diffraction/pomerons, and given hope that the internal structure of the pomeron can be probed. The experimental definition of a pomeron is an object that transfers energy and momentum, but no other quantum numbers like color or flavor. From this it follows that the pomeron is what causes elastic and diffractive scattering of hadrons in regions where the hadron remains intact. The best way to observe this kind of scatter is to use "Roman pots", which are small angle detectors capable of seeing an intact scattered proton. UA8 used these in conjunction with the UA2 calorimeter to detect dijet events in association with single diffractive scatters. This gave the initial hope that the pomeron had a definite partonic structure, which could be measured and described by perturbative QCD methods. All of the present measurements do not use Roman pots, but instead look for "rapidity gaps", which are meant to indicate a region of no particles and hence a colorless interaction. The HERA experiments are very close to adding Roman pots to their detectors as well, which in association with rapidity gaps will give very clean signatures for pomerons.

Now we'll describe the HERA and TEVATRON rapidity gap experiments. The HERA experiments discuss the gap in terms of the variable η_{max}, which is the maximum pseudorapidity of a calorimeter tower above a small energy threshold. The proton travels towards positive η, so as η_{max} gets smaller (including negative η) the gap between the proton and tower is larger and the rapidity gap (or particle-less region) is larger. Therefore smaller η_{max} means the interaction is more likely to arise from pomeron exchange rather than a normal QCD interaction. This is shown in figure 14 from the H1 experiment, where there is a sizeable excess of events with small η_{max} over the QCD prediction. In this plot there is no requirement that there be a dijet event, thus this could be normal single diffractive scattering that has been measured many times. The key thing to look for are dijet events in association with the rapidity gap, and an example of this is shown from the Zeus experiment in figure 15, where the jet transverse energy spectrum is displayed in events with $\eta_{max} < 2$. The spectrum compares well to predictions to models including pomeron production.

At the TEVATRON the experiments divide into two classes, the search for diffractive W production at CDF, which is similar to the HERA kinematics and looks for gaps at one end of the rapidity range, and the dijet events where the rapidity gap is searched for *between* the jets. In the dijet events one simply plots the number of charged tracks(CDF) or calorimeter towers(D0) above a small transverse energy threshold (300-400 MeV for both) in the region between the edges of the jet cones. This is shown in figure 16 for CDF and figure 17 for D0. Both experiments see an excess at small multiplicity above the extrapolated curve, indicating perhaps colorless exchange. The excess for all the CDF data is 6-7 standard deviations, while D0 has used a special gap trigger to improve its statistics and sees a 40 standard deviation effect. Both experiments define control regions in the data where they see no excess above the extrapolation. Neither experiment is claiming that these are signatures for pomeron exchange, and unfortunately neither have plans to add Roman pots soon, so the situation will remain somewhat murky. Hopefully the correlations measured at HERA between Roman pots and rapidity gaps can be used to improve the understanding of the TEVATRON measurements.

At this point nothing has indicated whether the pomeron has a gluon or quark structure from the measurements presented. To address this question a search for diffractive W production at CDF is presented, which should mostly come from quarks. If the possible hard quark structure of the pomeron is true, then we expect an enormous 17% of all Ws produced to come from diffractive processes. We note that the basic W cross section agrees with QCD predictions to within a few %, without the addition of diffractive Ws, thus this provides a constraint already. But diffractive Ws will have other distinctive features, the most notable being that the gap will be most of the time on the opposite side in η from the W. Thus if one looks for rapidity gaps on the side opposite to the W, there should be an excess of events to those where the gap is on the same side as the W. This is shown in figure 18, where the multiplicity distribution of calorimeter towers is shown for the two cases mentioned above. Diffractive Ws would show up as an excess in the first couple of bins in the opposite side events, and no excess is seen. This plus other features of these events have produced a measured fraction of diffractive Ws of 0.56 $\pm$ 1%, consistent with zero and far from the predictions of a hard quark pomeron.

7 Conclusions

As mentioned in the introduction, perturbative QCD is in excellent shape as a model of strong interactions. We see this in many different measurements. Some small technical deficiencies may be observed as the data sets become more precise, as perhaps shown with direct photons, but overall QCD describes the multitude of experiments extremely well. The boundaries of our understanding are also being pushed by the new kinematic regions (such as HERA) and new processes (hard diffraction) being probed. The next few years of investigation should prove to be very interesting for QCD.

References

[1] Siggi Bethke, *Proceedings of 22nd International Symposium on Physics with High Energy Colliders, 1994.*

[2] Paper in preparation, to be submitted to Physical Review.

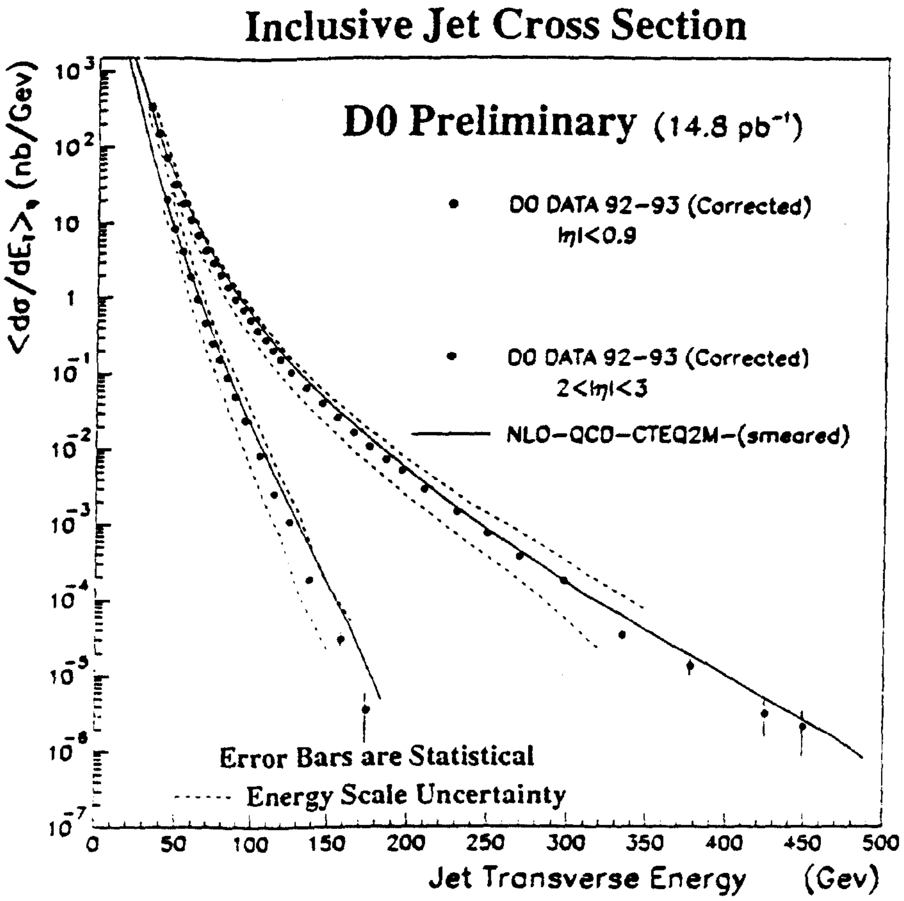

Figure 1: Inclusive jet cross sections from D0.

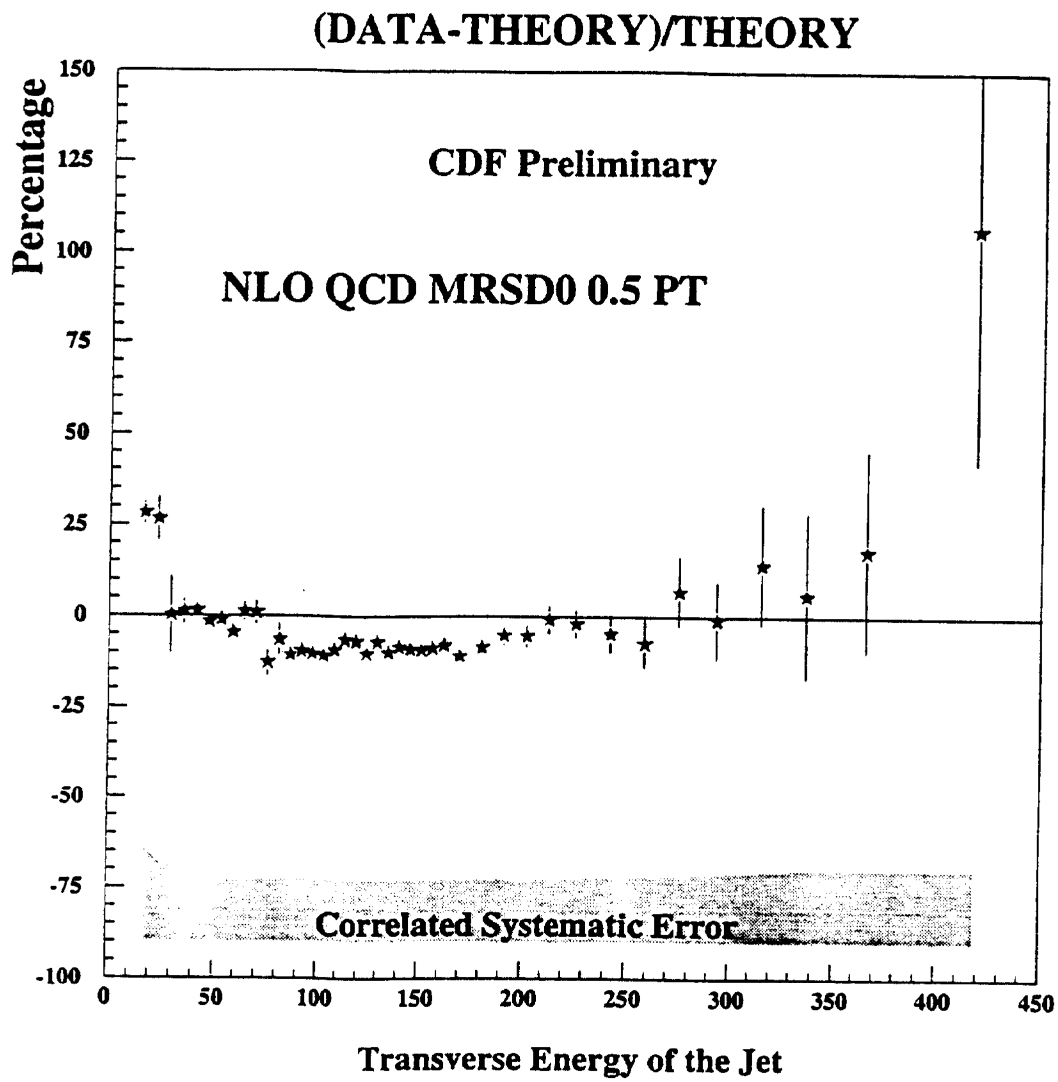

Figure 2: Inclusive jet cross section from CDF.

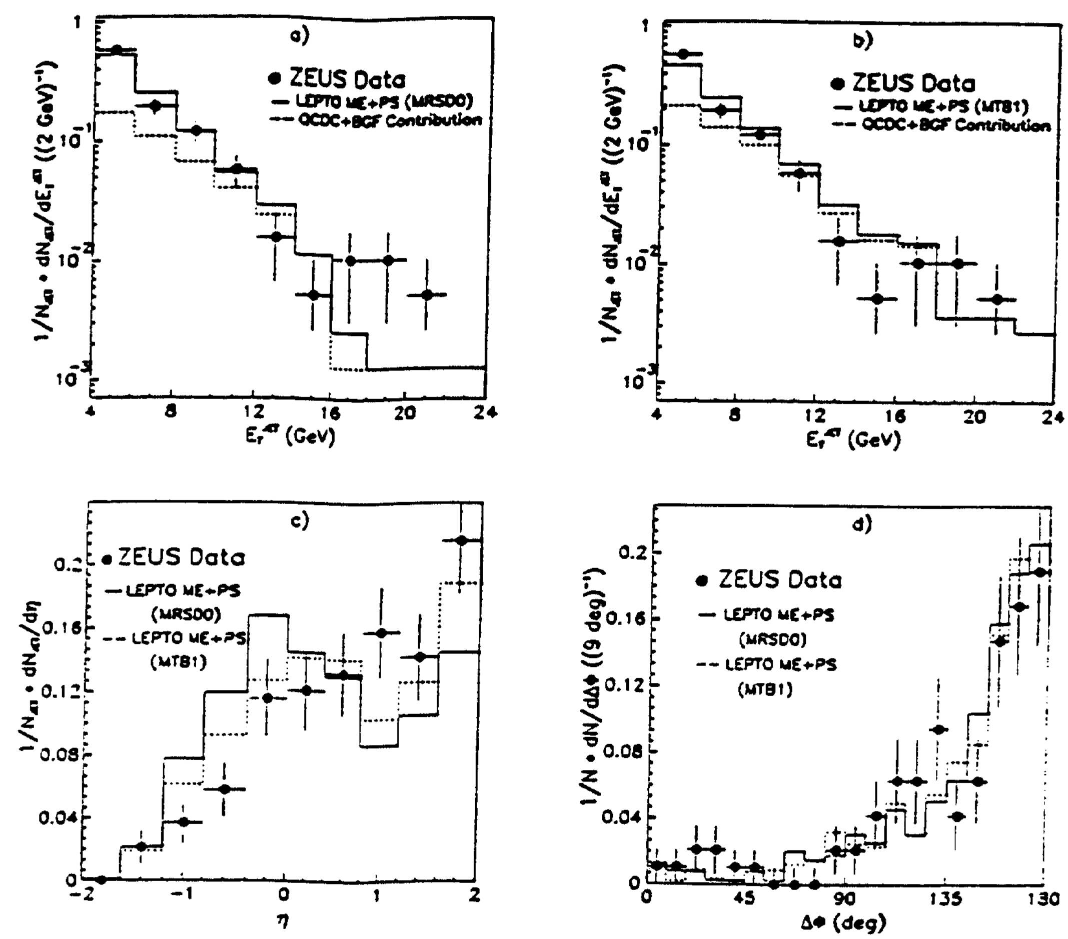

Figure 3: Two-Jet production at HERA.

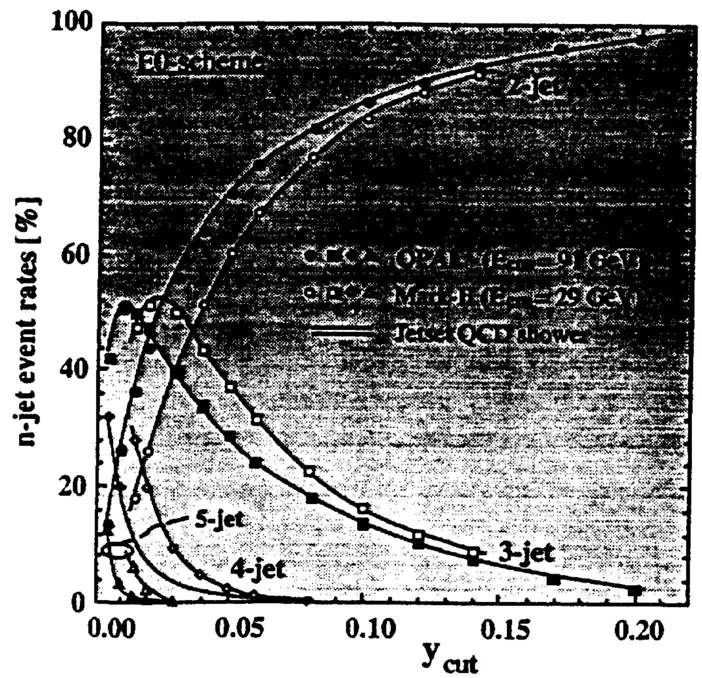

Figure 4: Jet fractions from LEP and PEP.

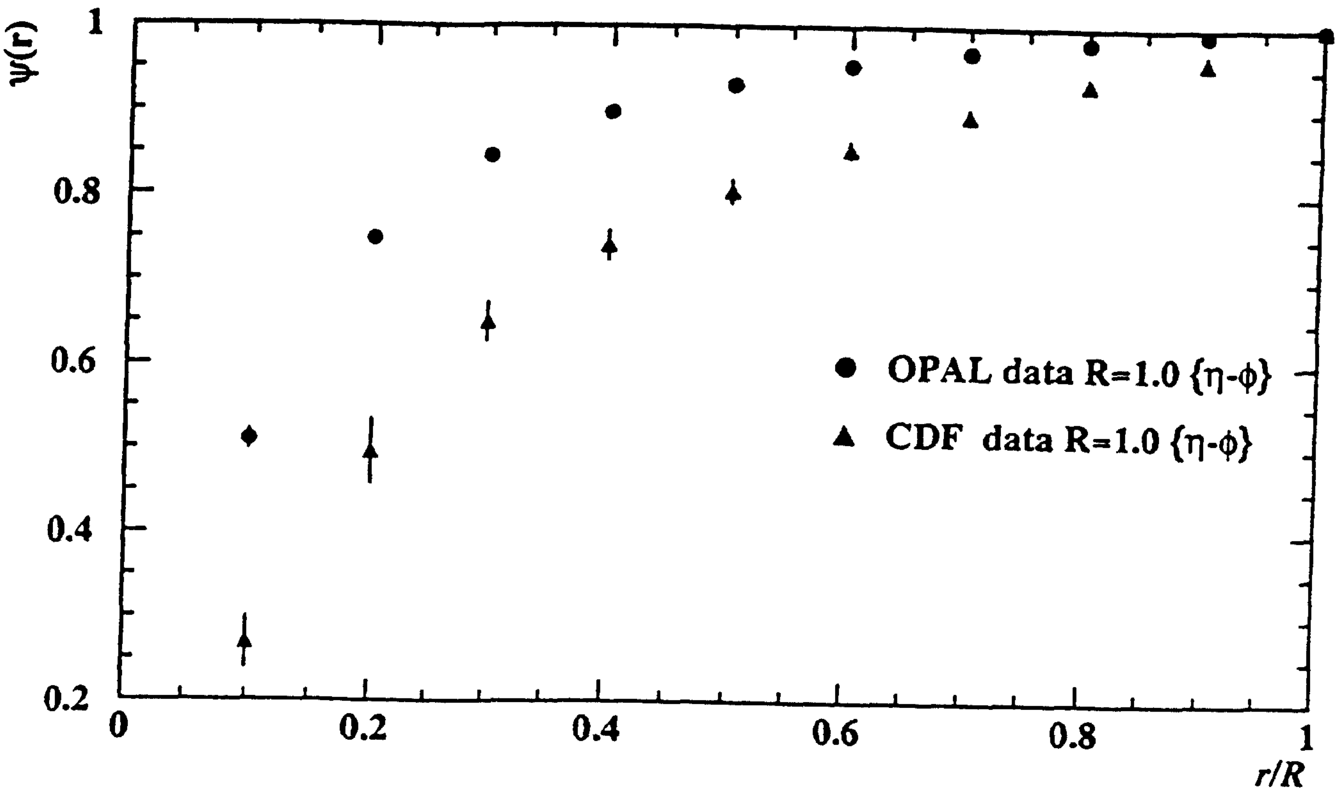

Figure 5: Jet shapes from OPAL and CDF, illustrating different shapes for quark and gluon jets.

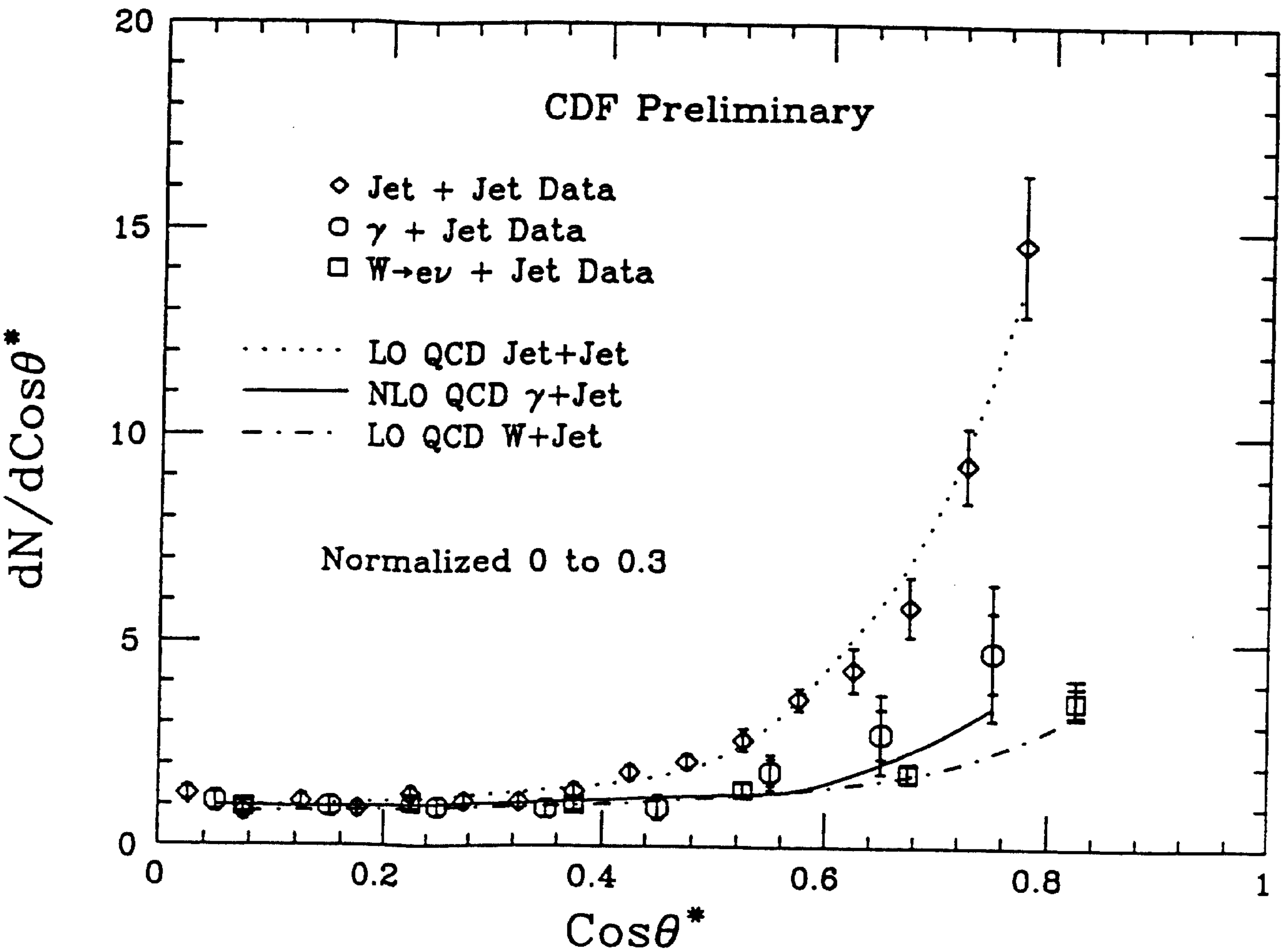

Figure 6: Dijet, photon, and W CM angular distributions from CDF.

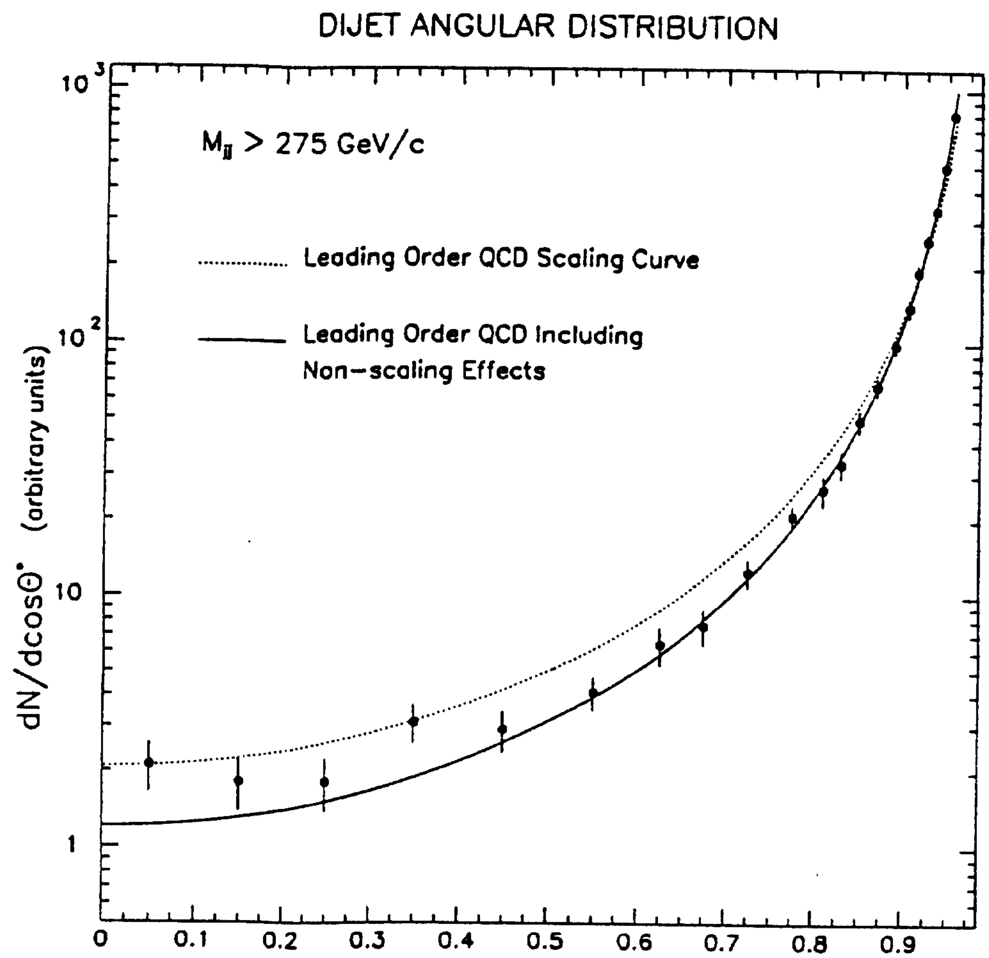

Figure 7: Dijet CM angular distribution from D0.

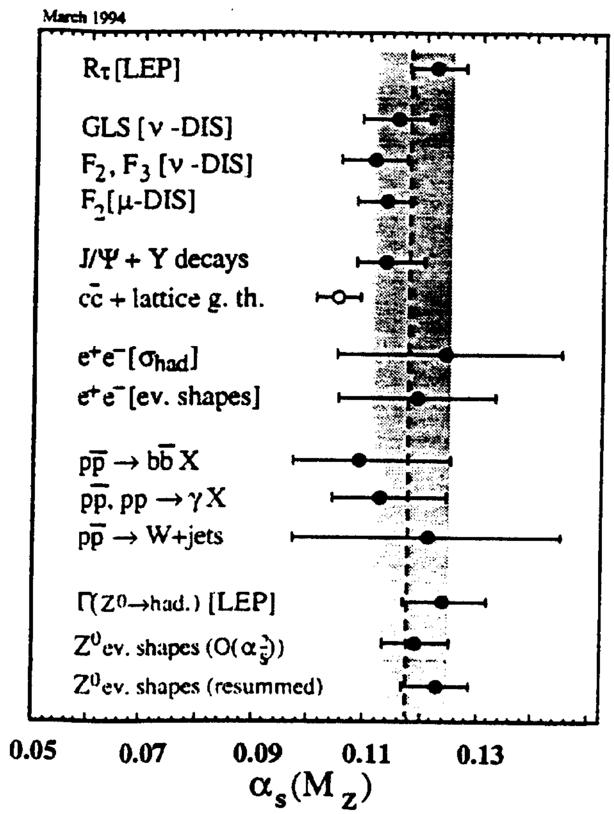

Figure 8: Summary of world's experiments on α_s.

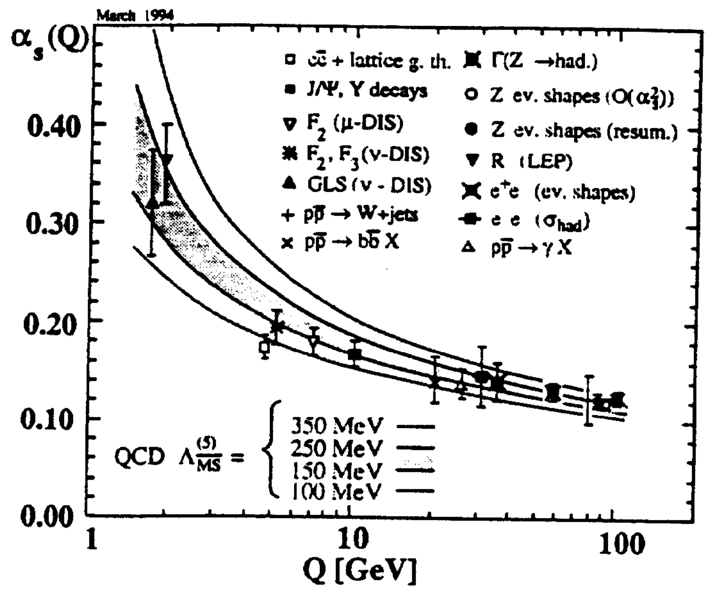

Figure 9: Different experiments displaying the running of α_s.

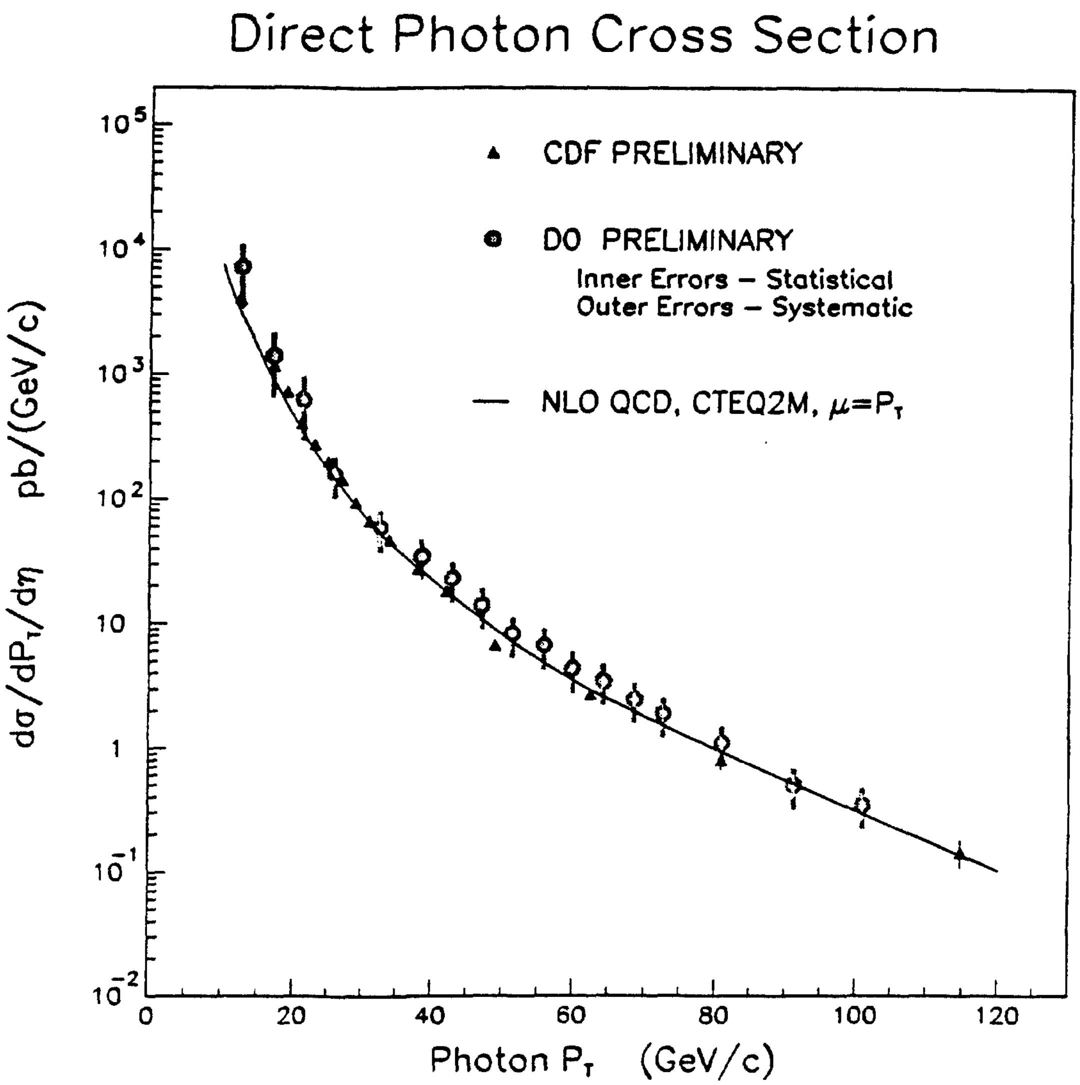

Figure 10: Direct photon production from CDF and D0.

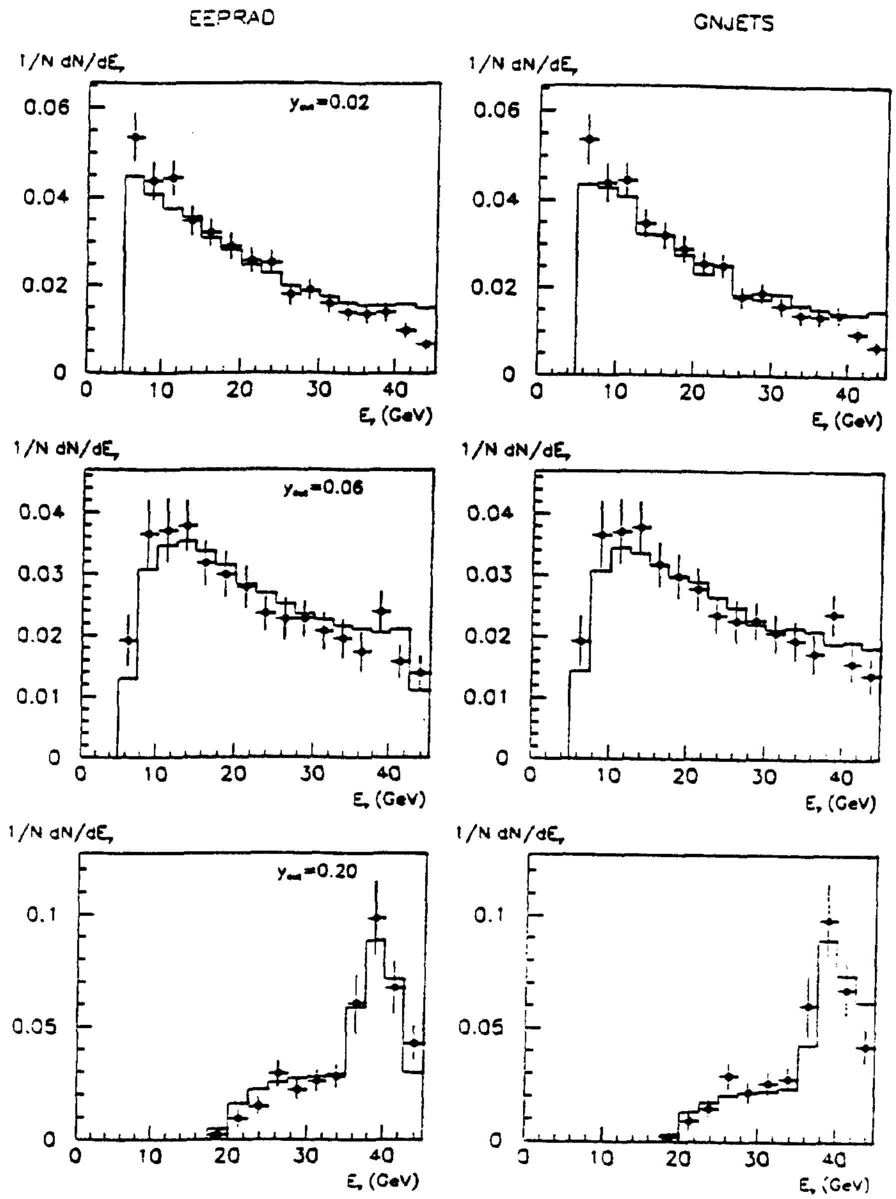

Figure 11: Photon production from OPAL.

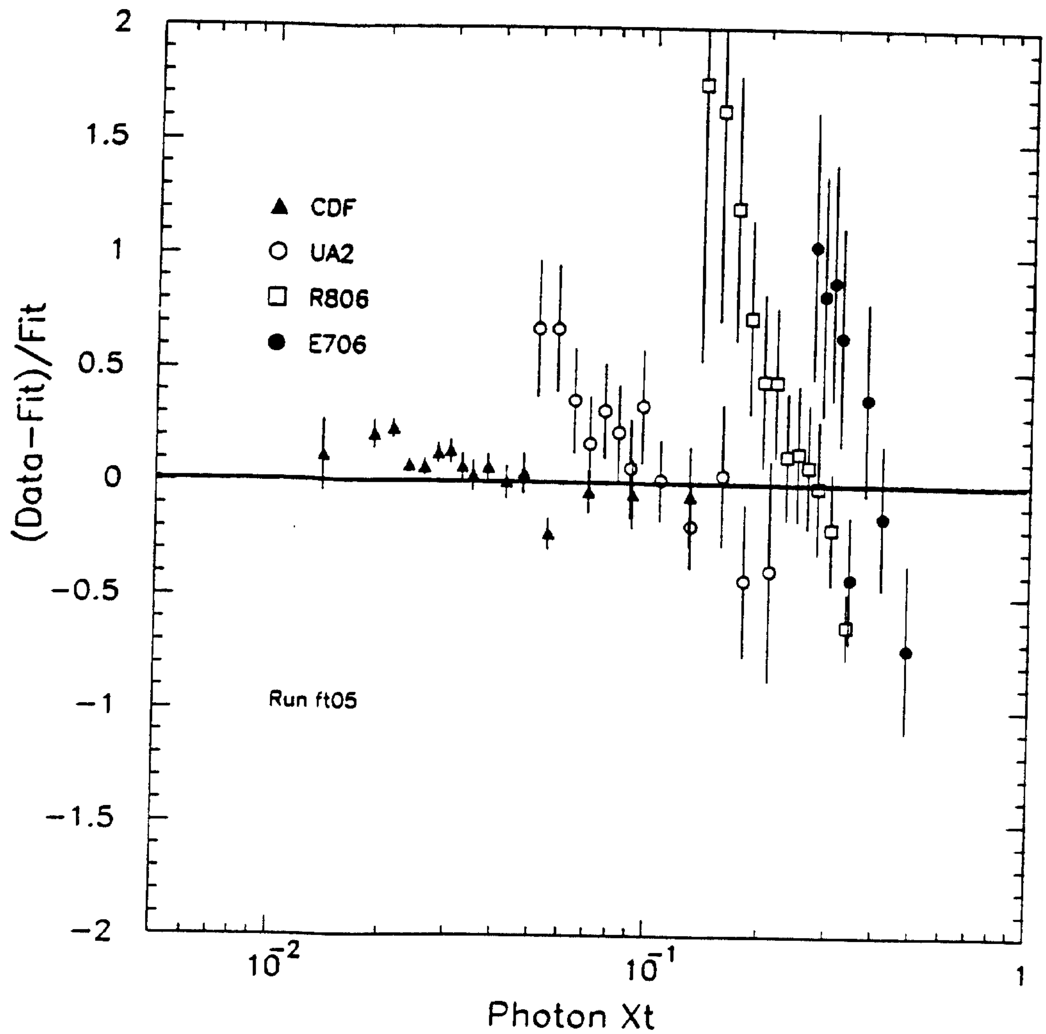

Figure 12: Compilation of different direct photon experiments compared to NLO QCD.

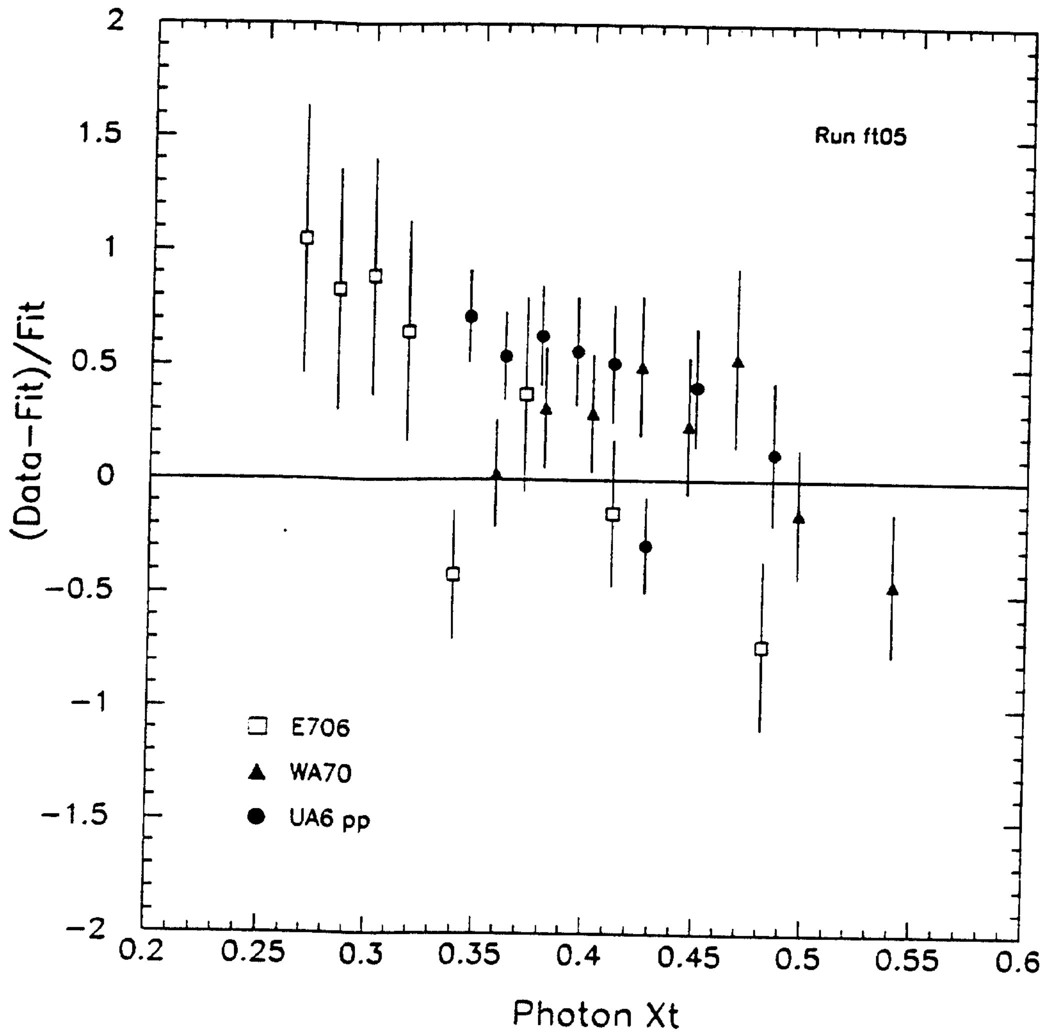

Figure 13: Fixed target experiments compared to NLO QCD.

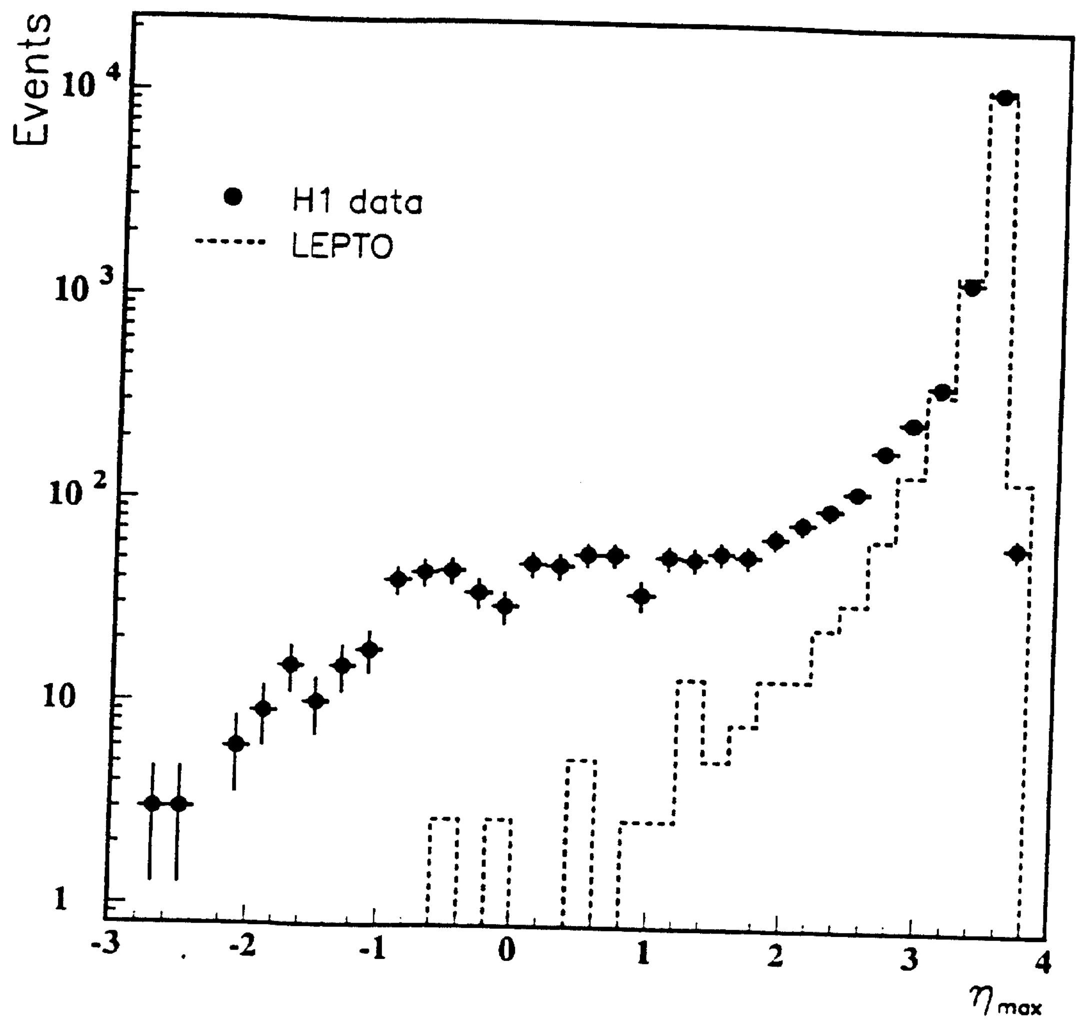

Figure 14: Rapidity gap measurement from H1.

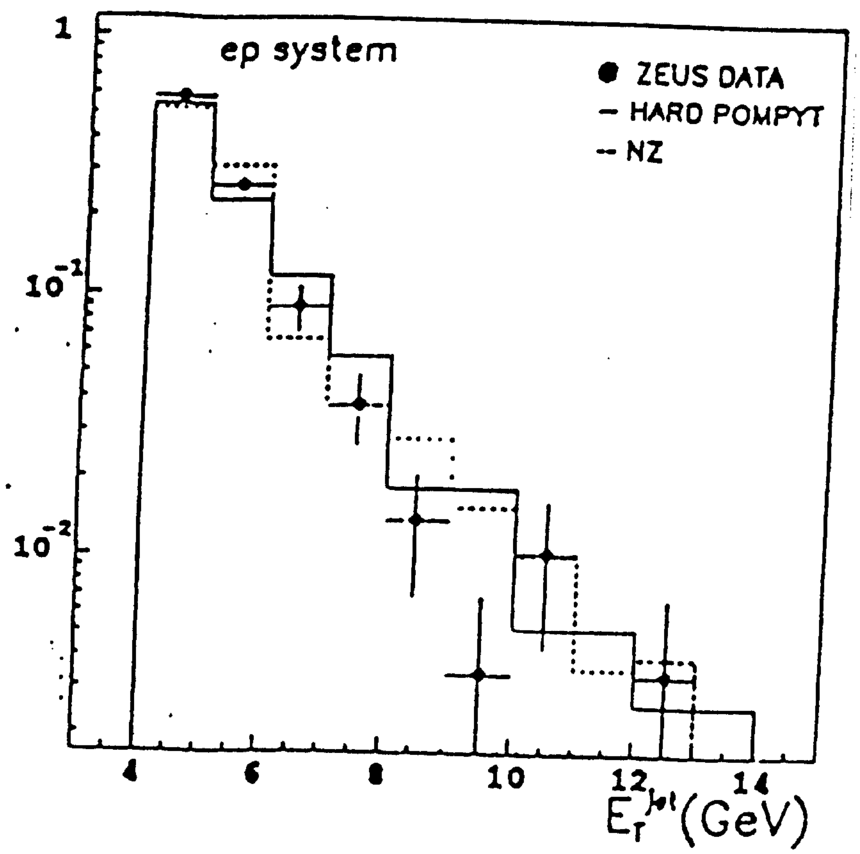

Figure 15: Jets in association with a rapidity gap as measured by Zeus.

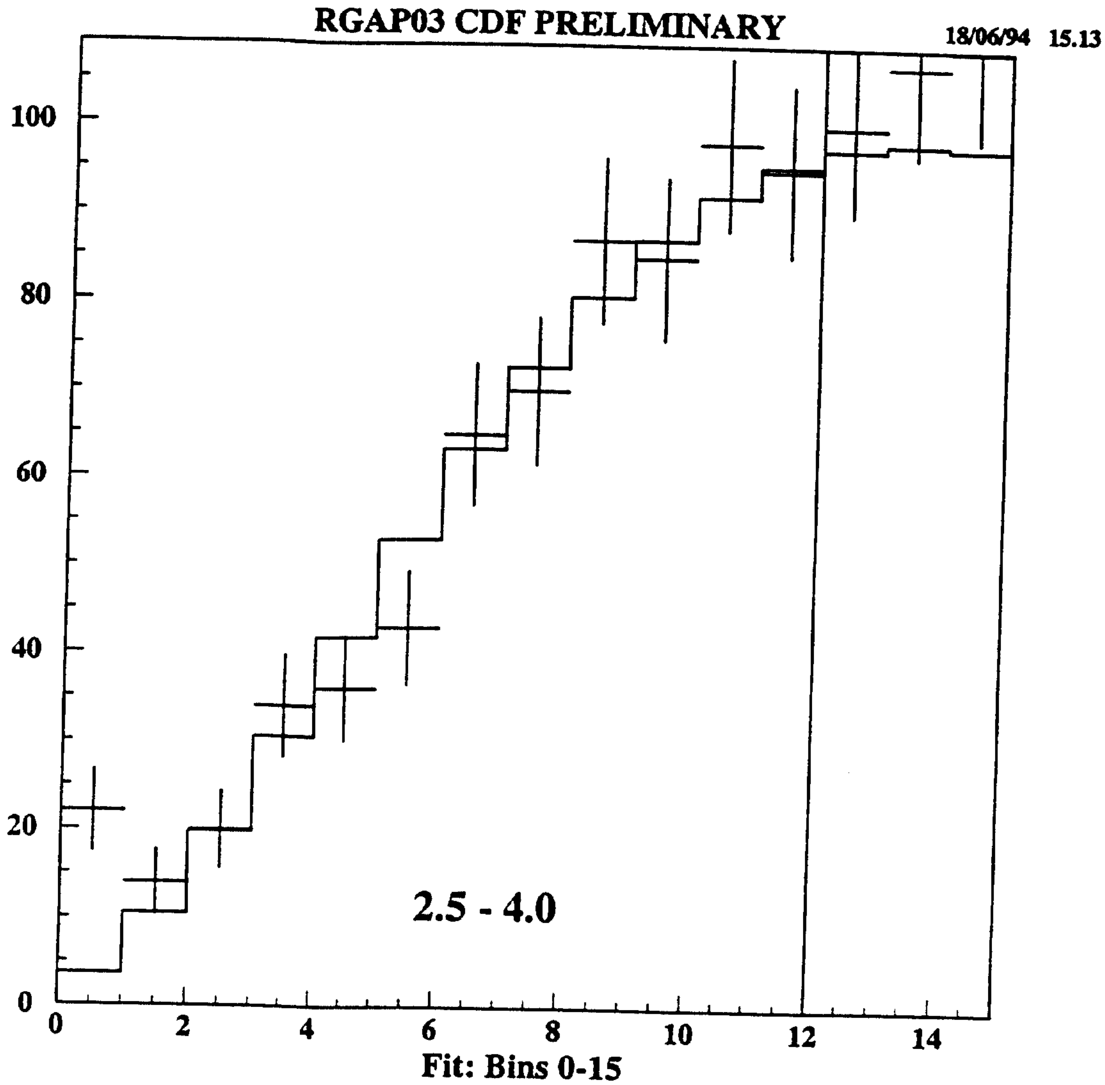

Figure 16: Rapidity gap measurement from CDF.

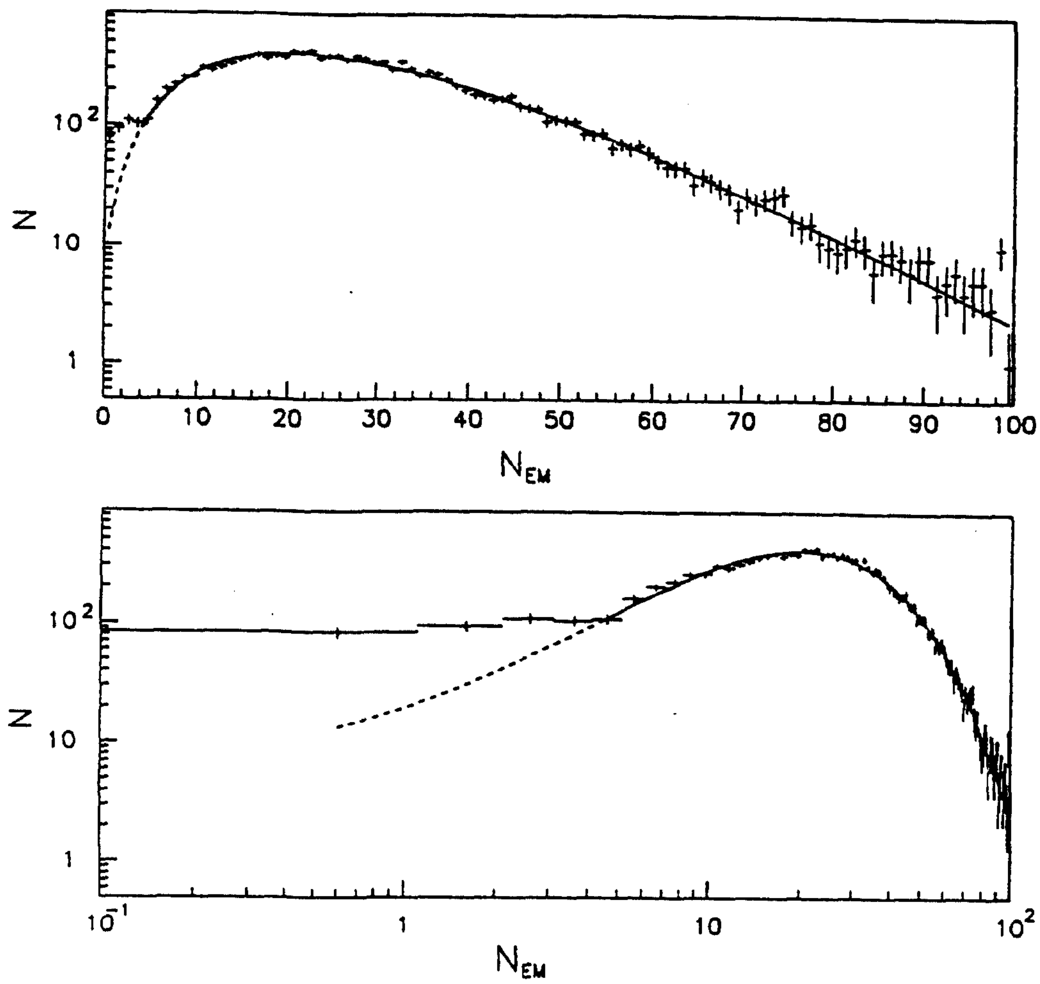

Figure 17: Rapidity gap measurement from D0.

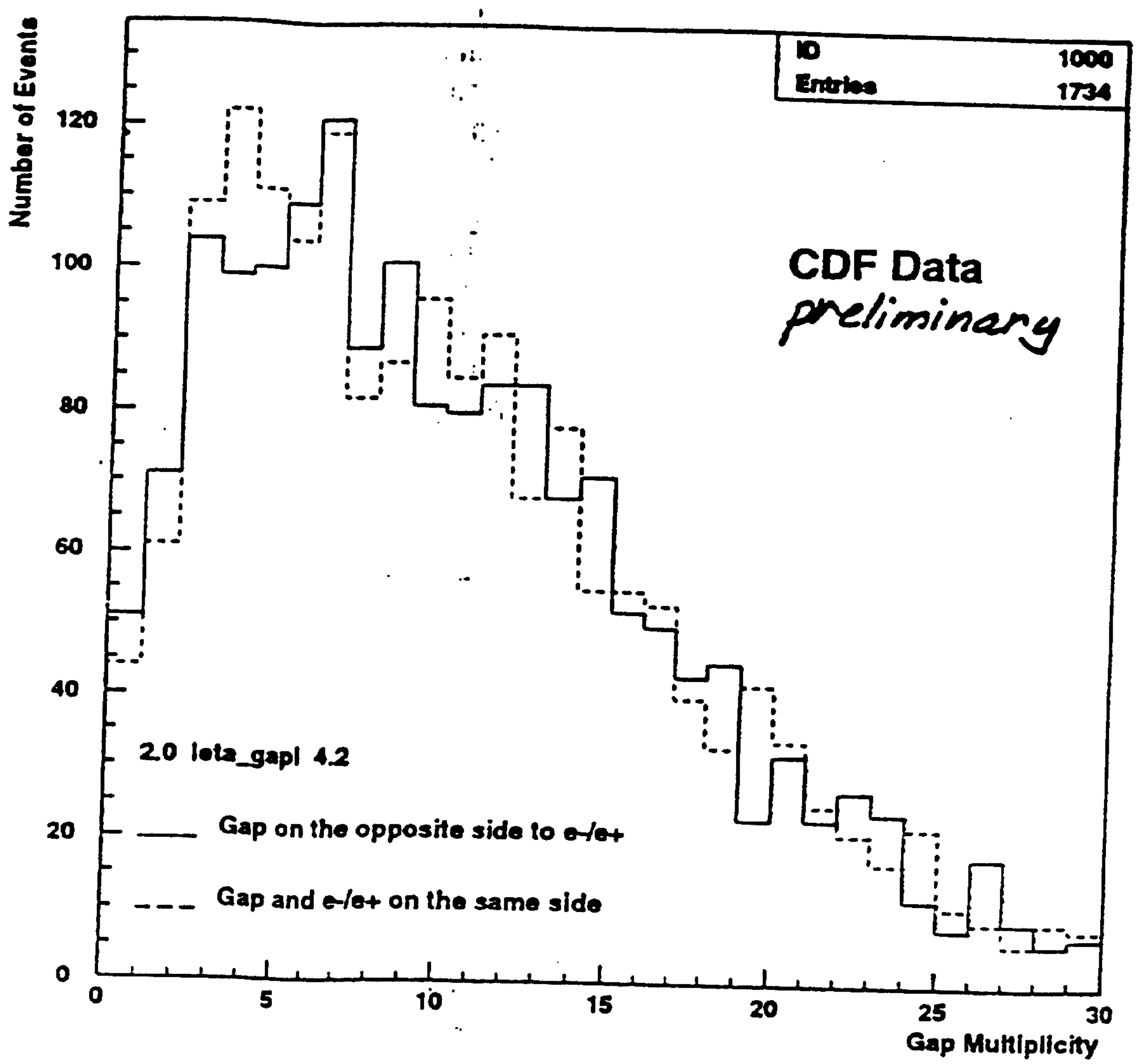

Figure 18: Search for Diffractive W production at CDF.